V European Conference on Computational Fluid Dynamics
ECCOMAS CFD 2010
J. C. F. Pereira and A. Sequeira (Eds)
Lisbon, Portugal,14-17 June 2010

NUMERICAL SIMULATION OF THERMAL CONVECTION UNDER THE INFLUENCE OF A MAGNETIC FIELD BY USING SOLENOIDAL BASES

Durmuş Yarımpabuç* [1] **and Hakan I. Tarman†**

*Department of Geology,
Süleyman Demirel University
Isparta, Turkey
e-mail: durmus@metu.edu.tr

†Department of Engineering Sciences
Middle East Technical University
06531 Ankara, Turkey
e-mail: tarman@metu.edu.tr

Key words: Thermal convection, Magnetic fields, Solenoidal Bases, Legendre Polynomials

Abstract. *The effect of a vertically imposed magnetic field on the thermal convection between rigid plates heated from below under the influence of gravity is numerically simulated in a computational domain with periodic horizontal extent. The numerical technique is based on solenoidal basis functions satisfying the boundary conditions for both velocity and induced magnetic field. Thus, the divergence-free conditions for both velocity and magnetic field are satisfied exactly. The expansion bases for the thermal field are also constructed to satisfy the boundary conditions. The governing partial differential equations are reduced to a system of ordinary differential equations under Galerkin projection and subsequently integrated in time numerically. The projection is performed by using a dual solenoidal bases set so that the pressure term is eliminated in the process. The quasi-steady relationship between the velocity and the induced magnetic field corresponding to the liquid metals or melts is used to generate the solenoidal bases for the magnetic field from those for the velocity field. The technique is validated first in the linear case by reproducing the marginal stability curves for varying Chandrasekhar number. Some numerical tests are performed in the nonlinear regime.*

[1] Currently at Engineering Sciences Department of Middle East Technical University

1 INTRODUCTION

In modeling incompressible flow, the flow field is restricted to satisfy the divergence-free condition or the continuity equation. This is an important hurdle to be overcome in the numerical simulation studies. For this purpose, various techniques have been employed in literature such as the fractional step[1], the influence matrix[2] and the staggered grid[3] methods. The common focus in these techniques is to numerically treat the pressure variable which usually comes without any boundary conditions and whose role is to enforce the divergence-free condition on the flow. On the other hand, these techniques help to enforce the divergence-free condition only to a certain limited degree of accuracy. Accurate handling of the divergence-free condition is important in numerical hydrodynamic stability studies where the flow is perturbed to identify the critical parameter values between the transitiory regimes. Furthermore, the numerical simulation studies of flow under the influence of a magnetic field encounter an additional divergence-free condition on the magnetic field variable. Various numerical approaches[4,5] have been used for this purpose and the effects of the poor handling of the divergence-free condition[6] and some remedies[7] are presented in literature.

In this work, we present some preliminary results on the use of solenoidal (divergence-free) bases expansion in the numerical simulation of thermal convection under the influence of a magnetic field in the vertical direction. By introducing an expansion in terms of solenoidal bases functions for the velocity and the magnetic field into the model equations in a Galerkin projection, both divergence-free criteria are exactly satisfied and the pressure variable is completely eliminated, thus the number of equations and the number of flow variables are reduced. This reduces the burden on the numerical technique and increases the accuracy with which the divergence-free condition is satisfied. While the velocity solenoidal basis functions are generated independently, a quasi-steady relationship between the velocity and the magnetic field variables is used to generate the corresponding magnetic solenoidal basis functions. This relationship arises in the case of liquid metals or melts as the convective fluid. Some studies that use solenoidal bases in literature are Busse & Clever[4], Leonard & Wray[8], Moser, Moin & Leonard[9], Mhuiris[10], Pasquarelli, Quarteroni & Sacchi[11], Kessler[12], Noack & Eckelmann[13], Meseguer & Trefethen[14] and Tarman[15].

2 GOVERNING EQUATIONS

Thermal convective motions of a perfectly conducting fluid is considered in a horizontal layer of thickness d between conducting plates that are heated from below under the influence of a uniform magnetic field B_0 applied externally in the vertical direction. The dimensionless form of the governing equations are

$$\nabla \cdot \mathbf{u} = 0, \tag{1}$$

$$\frac{\partial \mathbf{u}}{\partial t} + (\mathbf{u} \cdot \nabla)\mathbf{u} = -\nabla p + PrRa_h\Theta\mathbf{e}_z + Pr\nabla^2\mathbf{u} + Q_hPr(\mathbf{e}_z \cdot \nabla)\mathbf{b}, \tag{2}$$

$$\frac{\partial \Theta}{\partial t} + (\mathbf{u} \cdot \nabla)\Theta = \frac{1}{2}\mathbf{e}_z \cdot \mathbf{u} + \nabla^2 \Theta, \tag{3}$$

$$\nabla^2 \mathbf{b} = -(\mathbf{e}_z \cdot \nabla)\mathbf{u}, \tag{4}$$

$$\nabla \cdot \mathbf{b} = 0 \tag{5}$$

where $\mathbf{e}_z$ is the direction vector opposite to gravity, p the pressure, $\mathbf{u} = (u, v, w)$ the velocity vector, $\mathbf{b} = (b_x, b_y, b_z)$ the induced magnetic vector field and Θ is the deviation from the linear conductive temperature profile. The nondimensionalization is performed in accordance with Chandrasekhar[16] except for the length scale which is based on the half depth $d_h = \frac{1}{2}d$ for computational convenience. The resulting dimensionless numbers are the Rayleigh number Ra ($= 8Ra_h$), Chandrasekhar number Q ($= 4Q_h$) and Prandtl number Pr where

$$Ra = \frac{g \triangle T d^3 \alpha}{\kappa \nu}, \quad Q = \frac{B_0^2 d^2}{\rho \mu \nu \lambda}, \quad Pr = \frac{\nu}{\kappa}. \tag{6}$$

Magnetic field in the dimensionless form becomes

$$\mathbf{B} = \mathbf{e}_z + \frac{\kappa}{\lambda}\mathbf{b} \tag{7}$$

which indicates that the induced magnetic field $\mathbf{b}$ is weak compared to the externally imposed uniform magnetic field B_0 applied in the direction of $\mathbf{e}_z$ in a conducting fluid having the limit $\kappa \ll \lambda$ with κ and λ being thermal and magnetic diffusivities, respectively. Thus $\mathbf{b}$ can be viewed as a slaved variable prescribed by the velocity field as stated by the quasi-steady relationship (4). Liquid metals or melts are characterized by this limit.

We assume that the flow takes place in a doubly periodic three-dimensional rectangular region Ω in Fig. 1 with aspect ratio $s_x \times s_y \times 2$ or $\Gamma\left[\frac{1}{2}s_x : \frac{1}{2}s_y\right]$ such that

$$0 \le x \le s_x, \quad 0 \le y \le s_y, \quad -1 \le z \le 1, \tag{8}$$

where $s_x = L_x/d_h$ and $s_y = L_y/d_h$ are the dimensionless periods in the horizontal x and y directions, respectively. While periodic boundary conditions are used for all the dependent variables in the horizontal directions, the boundary conditions at the perfectly conducting plates in the vertical that are maintained at constant temperature take the form

$$\mathbf{u} = 0 \quad and \quad \frac{\partial b_x}{\partial z} = \frac{\partial b_y}{\partial z} = b_z = \Theta = 0 \quad at \quad z = \pm 1. \tag{9}$$

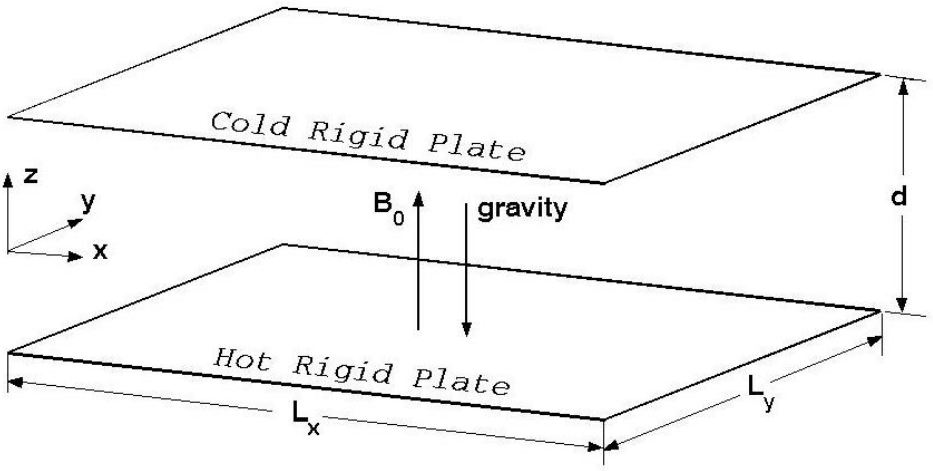

Figure 1: The geometry of the periodic convective domain

3 SOLENOIDAL BASIS

At the outset, the solenoidal basis functions $\mathbf{V}_p(\mathbf{x})$ are required to satisfy

$$\nabla \cdot \mathbf{V}_p = 0, \quad \mathbf{V}_p(\mathbf{x})\,|_{z=\pm 1} = \mathbf{0}. \tag{10}$$

The assumption of periodicity in the horizontal directions allows the use of Fourier representation

$$\mathbf{V}_p(\mathbf{x}) = \mathbf{V}_p(z) exp(ik_x x + ik_y y) \tag{11}$$

and reduces the continuity equation to the form

$$ik_x U + ik_y V + DW = 0 \tag{12}$$

where $\mathbf{V}(z) = (U, V, W)$ and $D = \frac{d}{dz}$ is the differentiation operator. It turns out that the basis functions come in pairs $\mathbf{V}_p^{(j)}(\mathbf{x})$, $j = 1, 2$ because the continuity equation reduces the degree of freedom in selecting the components of $\mathbf{V}_p(\mathbf{x})$ to two by connecting the three components together. A typical set of solenoidal basis functions are then:

$$\mathbf{V}_p^{(1)}(z) = \begin{bmatrix} -k_y g \\ k_x g \\ 0 \end{bmatrix}, \quad \mathbf{V}_p^{(2)}(z) = \begin{bmatrix} ik_x Dh \\ ik_y Dh \\ k^2 h \end{bmatrix} \tag{13}$$

with

$$\mathbf{V}_p^{(1)}(z) = \begin{bmatrix} g \\ 0 \\ 0 \end{bmatrix}, \quad \mathbf{V}_p^{(2)}(z) = \begin{bmatrix} 0 \\ h \\ 0 \end{bmatrix} \tag{14}$$

for $k_x = k_y = 0$. Here, $k^2 = k_x^2 + k_y^2$, $g = (1-z^2)L_p(z)$, $h = (1-z^2)^2 L_p(z)$ and $L_p(z)$ denotes Legendre polynomials. For the subsequent projection procedure, dual bases $\overline{\mathbf{V}}_p^{(j)}(\mathbf{x})$ need to be constructed to satisfy

$$\nabla \cdot \overline{\mathbf{V}}_p^{(j)} = 0, \qquad \overline{\mathbf{V}}_p^{(j)} \cdot \mathbf{e}_z \mid_{z=\pm 1} = 0. \tag{15}$$

It can be shown that these requirements on the dual basis causes the elimination of the pressure term $< \overline{\mathbf{V}}, \nabla p >$ in the projection procedure under the inner product

$$< \mathbf{f}, \mathbf{g} >= \int_{\Omega} \mathbf{f}^*(\mathbf{x}) \cdot \mathbf{g}(\mathbf{x})\, d\mathbf{x}. \tag{16}$$

A typical set of the dual bases can be constructed as in $(13-14)$ with $g = L_p(z)$, $h = (1-z^2)L_p(z)$.

Since the induced magnetic field $\mathbf{b}$ is prescribed by the velocity field as stated by the quasi-steady relationship (4), a solenoidal basis

$$\mathbf{B}(\mathbf{x}) = \mathbf{B}(z) exp(ik_x x + ik_y y) \tag{17}$$

for the magnetic field is constructed by solving

$$D^2\mathbf{B} - k^2\mathbf{B} = -D\mathbf{V}, \tag{18}$$

for $\mathbf{B}(z)$ subject to the boundary conditions

$$DB_x = DB_y = B_z = 0 \;\; at \;\; z = \pm 1. \tag{19}$$

for each $\mathbf{V} = \mathbf{V}_p^{(j)}(z)$ where $\mathbf{B}(z) = (B_x, B_y, B_z)$.

4 NUMERICAL EXPERIMENTS

The assumption of periodicity in the horizontal directions allows the use of Fourier series expansions of the dependent flow variables,

$$\begin{bmatrix} \mathbf{u} \\ \Theta \\ \mathbf{b} \end{bmatrix} (x,y,z,t) = \sum_m \sum_n \begin{bmatrix} \hat{\mathbf{u}} \\ \hat{\Theta} \\ \hat{\mathbf{b}} \end{bmatrix} (m,n,z,t) exp[i(\xi_m x + \eta_n y)] \tag{20}$$

where $\xi_m = \frac{2\pi m}{s_x}$ and $\eta_n = \frac{2\pi n}{s_y}$ are the wavenumbers with the ranges $1 - \frac{1}{2}N_x \le m \le \frac{1}{2}N_x$ and $1 - \frac{1}{2}N_y \le n \le \frac{1}{2}N_y$ for the indices m and n. The vertical profiles for velocity and the magnetic fields are further expanded in terms of the solenoidal bases

$$\hat{\mathbf{u}}(m,n,z,t) = exp(i\xi_m x + i\eta_n y) \sum_{p=0}^{M} a_p^{(1)}(t)\mathbf{V}_p^{(1)}(z) + a_p^{(2)}(t)\mathbf{V}_p^{(2)}(z), \tag{21}$$

$$\hat{\mathbf{b}}(m,n,z,t) = exp(i\xi_m x + i\eta_n y) \sum_{p=0}^{M} a_p^{(1)}(t)\mathbf{B}_p^{(1)}(z) + a_p^{(2)}(t)\mathbf{B}_p^{(2)}(z). \tag{22}$$

$$\tag{23}$$

The expansion for the thermal field is

$$\hat{\Theta}(m,n,z,t) = exp(i\xi_m x + i\eta_n y)\sum_{p=0}^{M} b_p(t)T_p(z), \tag{24}$$

where $T_p(z) = (1-z^2)L_p(z)$ with its dual $\overline{T}_p(z) = L_p(z)$. The evolution of the time dependent expansion coefficients $a_p^{(j)}(t)$ and $b_p(t)$ is determined by numerically integrating the projected governing equations in time. The velocity and magnetic fields share the same time evolution as dictated by the quasi-steady link stated in (4). For the numerical evaluation of the inner product integrals arising in the projection procedure, Gauss-Legendre-Lobatto (GLL) quadrature is used

$$< \mathbf{f}, \mathbf{g} >= \int_{-1}^{1} \mathbf{f}^*(z)\cdot\mathbf{g}(z)\,dz \approx \sum_{j=0}^{N_z} w_q \mathbf{f}^*(z_q)\cdot\mathbf{g}(z_q) \tag{25}$$

where (w_q, z_q) are GLL quadrature weights and nodes, respectively. It can be shown that associated with the GLL quadrature rules, the number of quadrature nodes N_z and the number of solenoidal basis M should be related in the least by $N_z = M + 4$ in order to render the numerical quadrature exact.

4.1 Linear Stability

In order to test the solenoidal basis and the projection procedure, we consider the linear stability of the conductive (no-motion) state leading to the critical values when the convective motion just sets in. The equations linearized around no-motion state

$$\frac{\partial \mathbf{u}}{\partial t} = -\nabla\Pi + PrRa_h\Theta\mathbf{e}_z + Pr\nabla^2\mathbf{u} + Q_h Pr(\mathbf{e}_z\cdot\nabla)\mathbf{b} \tag{26}$$

$$\frac{\partial \Theta}{\partial t} = \frac{1}{2}\mathbf{e}_z\cdot\mathbf{u} + \nabla^2\Theta \tag{27}$$

are projected onto the dual space after the introduction of the expansion in terms of the solenoidal basis resulting in a system of ordinary differential equations

$$\begin{bmatrix} \left\langle \overline{\mathbf{V}}_q^{(1)}, \mathbf{V}_p^{(1)} \right\rangle & 0 \\ 0 & \left\langle \overline{\mathbf{V}}_q^{(2)}, \mathbf{V}_p^{(2)} \right\rangle \end{bmatrix} \begin{bmatrix} da_p^{(1)}/dt \\ da_p^{(2)}/dt \end{bmatrix} = PrRa_h \begin{bmatrix} 0 & 0 \\ 0 & \left\langle \overline{\mathbf{V}}_q^{(2)}(z)\cdot\mathbf{e}_z, T_p \right\rangle \end{bmatrix} \begin{bmatrix} b_p \\ b_p \end{bmatrix}$$

$$+Pr \begin{bmatrix} \left\langle \overline{\mathbf{V}}_q^{(1)}, (-k^2+D^2)\mathbf{V}_p^{(1)} + Q_h D\mathbf{B}_p^{(1)} \right\rangle & 0 \\ 0 & \left\langle \overline{\mathbf{V}}_q^{(2)}, (-k^2+D^2)\mathbf{V}_p^{(2)} + Q_h D\mathbf{B}_p^{(2)} \right\rangle \end{bmatrix} \begin{bmatrix} a_p^{(1)} \\ a_p^{(2)} \end{bmatrix},$$

$$\left\langle \overline{T}_q, T_p \right\rangle db_p/dt = \frac{1}{2}\left\langle \overline{T}_q, \mathbf{V}_p^{(2)}(z)\cdot\mathbf{e}_z \right\rangle a_p^{(2)} + \left\langle \overline{T}_q, (-k^2+D^2)T_p \right\rangle b_p.$$

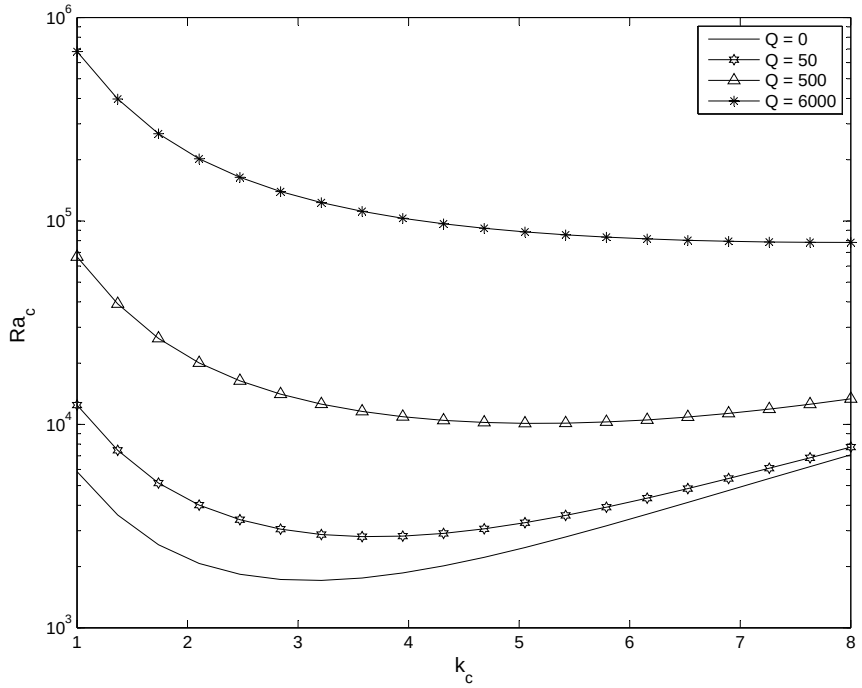

Figure 2: Ra_c versus k_c

		Chandrasekhar[16]	Present Work	Resolution
Q	k_c	Ra_c	Ra_c	$N_x \times N_y \times N_z$
0	3.12	1707.8	1707.8	$4 \times 4 \times 9$
50	3.68	2802.1	2802.1	$4 \times 4 \times 11$
500	5.16	10110.0	10110.0	$8 \times 8 \times 15$
6000	7.94	78391.0	78391.0	$8 \times 8 \times 25$

Table 1: Ra_c for various Q and wavenumber k_c

The assumption of a time dependence in the form

$$[a^{(1)}; a^{(2)}; b] \propto exp(\lambda t)$$

reduces the system to a generalized eigenvalue problem for the eigenvalues λ. The critical wave-number k_c and Rayleigh number Ra_c values for different Q values are listed in Table 1 for the rightmost eigenvalue just crossing the imaginary axis. These are obtained at the selection of $n = 0$ and $m = 1$ in (20). The corresponding marginal stability curve for increasing Q values is plotted in Figure 2. These are in agreement with the linear analysis in Chandrasekhar[16].

4.2 Nonlinear Regime

Fully nonlinear governing equations

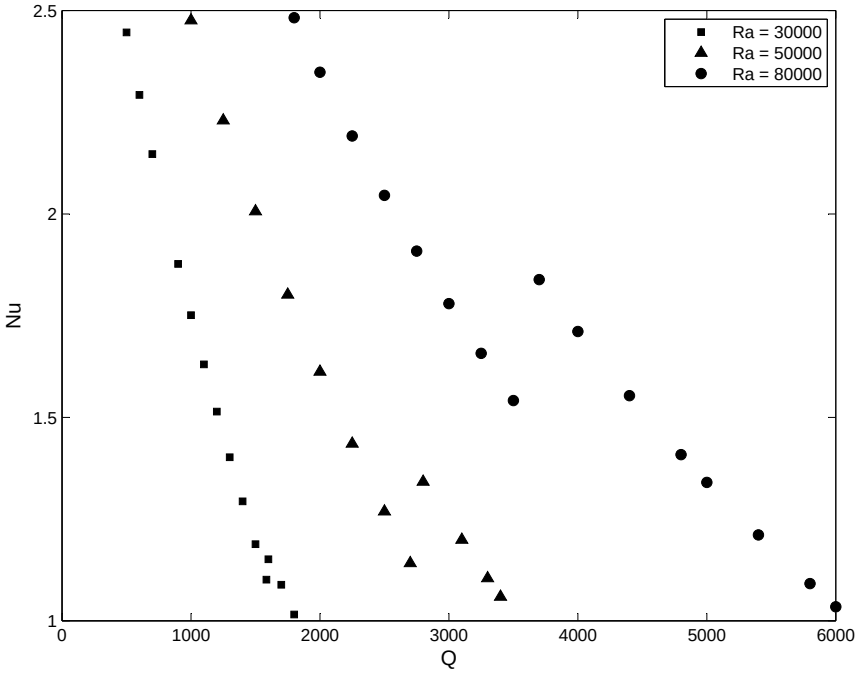

Figure 3: Nu versus Q for $Pr = 0.05$ at $\Gamma\,[3:1.5]$

$$\frac{\partial \mathbf{u}}{\partial t} + \mathbf{u} \times \mathbf{w} = -\nabla \Pi + PrRa_h \Theta \mathbf{e}_z + Pr\nabla^2 \mathbf{u} + Q_h Pr(\mathbf{e}_z \cdot \nabla)\mathbf{b}, \tag{28}$$

$$\frac{\partial \Theta}{\partial t} + (\mathbf{u} \cdot \nabla)\Theta = \frac{1}{2}\mathbf{e}_z \cdot \mathbf{u} + \nabla^2 \Theta \tag{29}$$

are discretized in time

$$(Pr\nabla^2 - \frac{2}{\triangle t})\mathbf{u}^{n+1} = \mathbf{g}^n, \tag{30}$$

$$(\nabla^2 - \frac{2}{\triangle t})\Theta^{n+1} = \mathbf{f}^n, \tag{31}$$

where

$$\mathbf{g}^n = -3(\mathbf{u} \times \mathbf{w} + PrRa_h \Theta \mathbf{e}_z + Q_h Pr(\mathbf{e}_z \cdot \nabla)\mathbf{b})^n$$
$$+(\mathbf{u} \times \mathbf{w} + PrRa_h \Theta \mathbf{e}_z + Q_h Pr(\mathbf{e}_z \cdot \nabla)\mathbf{b})^{n-1} - (Pr\nabla^2 + \frac{2}{\triangle t})\mathbf{u}^n, \tag{32}$$

and

$$\mathbf{f}^n = -3(\frac{1}{2}\mathbf{e}_z \cdot \mathbf{u} - (\mathbf{u} \cdot \nabla)\Theta)^n + (\frac{1}{2}\mathbf{e}_z \cdot \mathbf{u} - (\mathbf{u} \cdot \nabla)\Theta)^{n-1} - (\nabla^2 - \frac{2}{\triangle t})\Theta^n \tag{33}$$

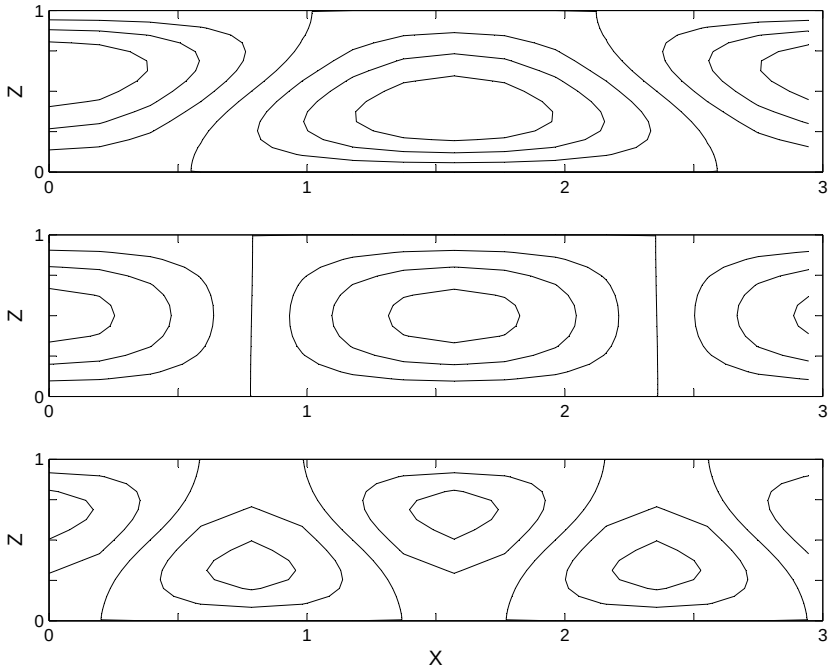

Figure 4: Temperature counters in the xz plane during the stages $t = 0, 30, 60$ of restructuring when initially $Q = 2500$ is suddenly set to 3000 at $Ra = 50000$, $Pr = 0.05$

using a semi-implicit scheme in which the non-linear advection and magnetic terms are treated explicitly using the second-order Adams Bashforth (AB2) method, and diffusion terms are discretized using an implicit Crank Nicolson (CN) scheme. This results in a second-order accurate scheme in time. The resulting weak form of these equations after the projection procedure is used to obtain the time evolution of the expansion coefficients.

The numerical experiments are performed to study the effects of varying Q (magnetic field strength) on the convective heat transport efficiency indicated by Nusselt number (Nu) at selected Ra values. A liquid metal with $Pr = 0.05$ is selected in a layer with aspect ratio $\Gamma\,[3 : 1.5]$ and subjected to a vertical magnetic field. The computation is started with the flow field just supercritical obtained using the eigenfunctions of the previous linear stability study. It is known that application of a vertical magnetic field suppresses the convective motions as shown in Figure 3 by decreasing Nu values as Q increases, ultimately approaching to the conductive state with $Nu = 1$. In the process, kinks appear at $Q = 1400$ for $Ra = 30000$, at $Q = 2500$ for $Ra = 50000$ and at $Q = 3600$ for $Ra = 80000$. The kinks coincide with the increase in the number of rolls and thus decrease in the wavelength. This is also observed and discussed in an earlier numerical study[17]. This change in the roll pattern is shown in Figure 4 when $Q = 2250$ is increased to $Q = 3000$ for $Ra = 50000$ at the transient stages $t = 0, 30, 65$. All these runs are in the steady roll motion regime and use a typical dimensionless time step between 10^{-3} and 10^{-4}.

Acknowledgements

This study was supported by the Scientific and Technical Research Council of Turkey (TÜBİTAK) through research project 109M435.

REFERENCES

[1] Orszag, S.A. and Kells, L.C., Transition to turbulence in plane Poiseuille flow and plane Couette flow, *J. Fluid Mech.*, **96**, 159–205 (1980).

[2] Kleiser, L. and Schumann, U., Treatment of incompressibility and boundary conditions in 3-D numerical spectral simulations of plane channel flows, in Hirschel, In proceedings of the *E.H. (ed.): Third GAMM Conference on Numerical Methods in Fluid Mechanics*, Vieweg, Braunschweig, 165–173 (1980).

[3] Canuto, C., Hussaini, M.Y., Quarteroni, A. and Zang, T.A., Spectral Methods: Evolution to Complex Domains and Applications to Fluid Dynamics, *Springer, New York*, (2007).

[4] Busse, F.H. and Clever, R.M., Stability of convection rolls in the presence of a vertical magnetic field, *Phys. Fluids*, **25**, 931–935 (1982).

[5] Mössner, R. and Müller, U., A numerical investigation of three dimensional magneto convection in rectangular cavities, *Int. J. Heat Mass Transf.*, **42**, 1111–1121 (1999).

[6] Brackbill, J.U and Barnes, D.C., The effect of nonzero divergence on the numerical solution of the MHD equations, *J. Comp. Phys.*, **35**, 426–430 (1980).

[7] Balsara, D.S. and Kim, J., A comparison between divergence-cleaning and staggered-mesh formulations for numerical magnetohydrodynamics, *Astrophysical Journal*, **602**(2-I), 1079–1090 (2004).

[8] Leonard, A. and Wray, A., A new numerical method for the simulation of three-dimensional flow in a pipe, *NASA Technical Memorandum*, (1982).

[9] Moser, R. D., Moin, P., and Leonard, A., A spectral numerical method for the Navier-Stokes equations with applications to Taylor-Couette flow, *J. Comput. Phys.*, **52**, 524–544 (1983).

[10] Mhuiris, N.M.G., The construction and use of divergence free vector expansions for incompressible fluid flow calculations, *NASA Technical Memorandum*, (1986).

[11] Pasquarelli, F., Quarteroni, A., and Sacchi-Landriani, G., Spectral approximations of the Stokes problem by divergence-free functions, *J. Sci. Comput.*, **2**, 195–226 (1987).

[12] Kessler, R., Nonlinear transition in three-dimensional convection, *J. Fluid Mech.*, **174**, 357–379 (1987).

[13] Noack, B.R. and Eckelmann, H., A low-dimensional Galerkin method for the three-dimensional flow around a circular cylinder, *Phys. Fluids*, **6**(1), 124–143 (1994).

[14] Meseguer, A. and Trefethen, L.N., Linearized pipe flow to Reynolds number 10^7, *J. Comp. Phys.*, **186**, 178–197 (2003).

[15] Tarman, I. H., Reduced order modeling of thermal convection under a magnetic field, In proceedings of the *European Conference on Computational Fluid Dynamics*, WCCM8 - ECCOMAS 2008.

[16] Chandrasekhar, S., Hydrodynamics and Hydromagnetic Instability, *Oxford: Clarendon Press*,(1961).

[17] Güray, E. and Tarman, I. H., Thermal convection in the presence of a vertical magnetic field, *ACTA Mechanica*, **194**, 33–46 (2007).